Adsorption energies of H and H_2: a quantum-chemical study*

Milan Sil[1], Prasanta Gorai[1], Ankan Das[1,a], Dipen Sahu[2,1], and Sandip K. Chakrabarti[3,1]

[1] Indian Centre for Space Physics, 43, Chalantika, Garia Station Road, 700084 Kolkata, India
[2] Atomic Molecular and Optical Spectroscopy Division, Physical Research Laboratory, 380009 Ahmedabad, India
[3] S. N. Bose National Centre for Basic Sciences, Salt Lake, 700098 Kolkata, India

Abstract. The chemical composition of interstellar grain mantle is mostly dependent on adsorption energies of the surface species. Since hydrogen is widespread either in atomic or in molecular form, our aim in this work is to review (by quantum chemical calculations) the variation of the adsorption energies of H and H_2 depending on the nature of the adsorbents. Choice of absorbents was based on relative abundances of interstellar materials. Since carbonaceous and silicate grains are very abundant, we used them as our absorbents. To save computational time, benzene (smallest structure sample of PAHs) is employed as carbonaceous material and for silicate grain, simple cluster of silicon dioxide (silica) $(SiO_2)_3$ is used. Around dense cloud regions, water is the major constituent of a grain mantle, therefore, usage of binding energies with bare grains is immaterial. To mimic the water as the adsorbents, we use a water-cluster $((H_2O)_6)$. We found that, for all types of adsorbents considered here, binding energies of H are always lower than those of H_2, whereas, some of the experimental values are just the other way around. Assuming a steady state solution to the rate equation method, we also present the H_2 formation efficiency window in various cases.

1 Introduction

Adsorption energy of surface species is the key to study formation of complex molecules on interstellar grain surfaces. Hydrogen is the most abundant element in the universe and mainly exists in two forms, namely, atomic (H) and molecular (H_2). H_2 is believed to be a precursor of more complex molecules. One of its protonated forms, namely, H_3^+ acts as an important coolant and saves itself along with other species from incoming radiation fields [1]. Most of the complex molecules are produced during these cold stages of the star formation. There are various studies on regarding the formation of complex molecules during star formation [2–15]. The process of formation molecular hydrogen through gas-phase interactions between hydrogen atoms (or ions) is too slow compared to the observed formation rate [16]. Therefore it is commonly believed that there must be other processes causing rapid formation of molecular hydrogen. H_2 may be formed by taking two hydrogen atoms and putting them together. But in the gas phase, the probability of two hydrogen atoms finding each other is much smaller than that of one single hydrogen atom finding a larger grain. So a suitable larger grain surface may accrete many simple species (atoms or molecules). There are two types of adsorption: (a) physisorption or molecular adsorption, and (b) chemisorption or dissociative adsorption. Interstellar grains play an essential role in formation of molecules at low temperature regime [17] and physisorption is always favoured at low temperatures. Incoming H atoms can stick with grain surfaces and form molecules via different mechanisms: (i) Langmuir-Hinshelwood (LH) mechanism, where two species can adsorb and react on neighbouring sites [18]; (ii) Eley-Rideal (ER) mechanism, where formations can happen by direct impingement of incoming species on an adsorbed species [19,20] and (iii) Hot-atom mechanism [21], where the incoming species with large impact parameters may be trapped and react with other adsorbed species. Formation of molecular hydrogen on the grain surface has already been discussed by various authors [16,22–26]. Details of such formation provide a valued information about the physical and chemical evolution of the space environments. Because of its higher abundances, molecular hydrogen (H_2) clearly dominates the spectral characteristics of molecular clouds in the FUV and near-IR region [16].

The exact composition of the dust grains remains unknown, although there is a strong evidence that they are composed of carbonaceous or siliceous material [17,27–29]. Polycyclic aromatic hydrocarbons (PAHs) are thought to be a good candidate for the main component of carbonaceous dust grains [27,29]. The presence of graphite in the interstellar medium is supported by observations

* Contribution to the Topical Issue "Low-Energy Interactions related to Atmospheric and Extreme Conditions", edited by S. Ptasinska, M. Smialek-Telega, A. Milosavljevic and B. Sivaraman.

[a] e-mail: ankan.das@gmail.com

of extinction nature with a wavelength of around 200 nanometers [16]. Depending on the region, the grains may also be covered with ice. In fact, interstellar dust plays an essential role of having a high abundance of molecular hydrogen in the ISM [25,26,30–32] and some significant fractions of the interstellar complex molecules would be synthesized on interstellar dusts [33–36]. References [37,38] already had shown the importance of surface chemistry for H_2-formation, where dust grains were found to catalyze the process. Experiments on models of these grains and investigations of their impacts on chemistry under conditions of interstellar medium (ISM) were carried out by various authors [39–42]. Since the spacing between the layers in graphite is large, one may assume that calculations including a single graphene sheet (one layer of graphite) may provide satisfactory results. Several computational studies (quantum chemical and molecular dynamics) were carried out ($C_{24}H_{12}$) [43–46] to model graphene surface.

Plan of this paper is as follows. In Section 2, computational details and methodology are discussed. In Section 3, calculation of binding energies are discussed. In Section 4, chemical modeling on the formation of H and H_2 is explained and finally, in Section 5, we draw our conclusions.

2 Computational details and methodology

All the calculations reported in this paper are carried out using Gaussian 09 suite of programs [47]. Second-order Møller-Plesset (MP2) method and aug-cc-pVDZ basis are included in computing the optimized energy of all the structures. "Aug" prefix is used to add diffusion function and cc-pVDZ is the Dunning's correlation consistent basis set [48] having double zeta function. Fully optimized structure is verified to be a stationary point (having non-negative frequency) by harmonic vibrational frequency calculations and all the calculations are performed without zero point energy corrections. The adsorption energy of a species on the grain surface is calculated as follows:

$$E_{ads} = E_{ss} - (E_{surface} + E_{species}), \quad (1)$$

where, E_{ads} is the adsorption energy, E_{ss} is the optimized energy for species placed at a suitable distance from the grain surface, $E_{surface}$ and $E_{species}$ are the optimized energies of the grain surface and species respectively.

A general scheme for calculating the adsorption energy of non-polar molecules on a graphite surface was already being discussed in [49,50]. We also employed their relation to coming up with an educated estimation of the binding energies of H and H_2. As the input parameters, polarizability and diamagnetic susceptibility of H and H_2 are supplied by using quantum chemical calculations with B3LYP/6-311g(d,p) method. For the placement of the adsorbed species on the lattice of graphite, we have used three different positions as mentioned in reference [51]. First, over the carbon atom (position c); second, over the mid-point between two neighbouring carbon atoms (position b); and finally, over the center of the hexagon

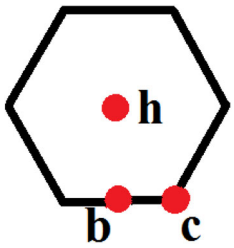

Fig. 1. Three favourable positions, c, h and b are shown. c position is at the top of a carbon atom, h (hollow) position is at the center of the hexagon and b (bridge) position is at the mid-point between two adjacent carbon atoms.

Table 1. Binding energy of H and H_2 using the method used in [49].

Species	Adsorption energy for h position (Kelvin)	Adsorption energy for b position (Kelvin)	Adsorption energy for c position (Kelvin)
H	268	171	157
H_2	944	594	545

of carbon atoms (position h). A schematic arrangement of hydrogen atoms on the simple unit of PAH molecule (benzene) for these three different positions is shown in Figure 1.

References [49,50] considered that hydrogen atom and molecule are sticking with the graphite as an adsorbent. They calculated the adsorption energy (Φ_i'') of a segment of i of adsorbate atom by,

$$\Phi_i''(z) = -C_{i1}p_1 z^{-q_1} - C_{i2}p_2 z^{-q_2} - C_{i3}p_3 z^{-q_3} + B_i'' p_m z^{-q_m} \quad (2)$$

where, B_i'' is the constant associated with the repulsion, z is the distance from the ith segment, p_1, q_1, p_2, q_2, p_3, q_3, p_m, q_m are the constants available from the logarithmic graphs of [49,50] and C_{i1}, C_{i2} and C_{i3} are the constants. For the computation of C_{i1}, C_{i2} and C_{i3}, polarizability and diamagnetic susceptibility of the adsorbate and adsorbent are required. Since we choose graphite as the adsorbent, we use the values given in [51] for the individual carbon atom (polarizability $= 0.937 \times 10^{-24}$ cm^3 and diamagnetic susceptibility $= -10.54 \times 10^{-30}$ cm^3). For the adsorbates, we have calculated the polarizability and diamagnetic susceptibility by using Gaussian 09 software. We have obtained the values of mean polarizability 8.742887×10^{-26} cm^3 for H atom and 4.48999×10^{-25} cm^3 for H_2 molecule and diamagnetic susceptibility of $-4.07199302 \times 10^{-30}$ cm^3 for H atom and -6.0225×10^{-30} cm^3 for H_2 molecule.

Using the above-mentioned method, we have calculated the adsorption energy of H and H_2 on graphite grain surface for various positions. From Table 1, it is clear that the most favorable adsorption occurs at the hollow (h) site which [50] had mentioned earlier. We have done additional calculations using the method presented by these authors in order to compare with our own calculated results discussed in the next sections.

3 Results and discussions

Adsorption of species on the grain surface is the primary process for any molecular formation mechanism and H and H_2 being most abundant it is essential to know their adsorption energies for various substrates. Since binding energies of the surface species mainly control surface chemistry, using an inaccurate estimation may cause totally deceptive results. In this section, we report the results of our high-level quantum chemical calculations for the adsorption energies of H and H_2. Here, we use three types of substrate as the grain materials: (i) benzene surface; (ii) silica cluster and (ii) water cluster.

3.1 Benzene surface

The chemistry of hydrogen-graphite and hydrogen-PAHs systems are considered to be realistic models to investigate molecular hydrogen formation in the ISM. Here, we consider benzene to model graphite, graphene, or PAHs. Here, our main goal is to find out the trend of binding energy between the hydrogen atom and hydrogen molecule for various types of grain surfaces. Reference [44] found that the binding energy of hydrogen atom is 18.8 meV with the most favorable hollow site of benzene surface (MP2 method was implemented along with the Aug-cc-pVDZ basis set). Reference [44] also carried out their calculation for the much higher level quantum chemical calculation (CCSD method) by considering the same basis set. They obtained the adsorption energy of H atom to be 18.7 meV with the CCSD method. Resulting differences between the MP2 and CCSD method for this system was thus negligible in the broader astrophysical aspects. Thus to save the computational time, we also have employed MP2/Aug-cc-pVDZ level of theory for our calculations. Similar method and basis set is also employed for the computation of adsorption energy of H_2. Although coronene surface is best suited to mimic the interstellar grain, we use benzene surface to save the computational time. Benzene is a vital organic compound having the chemical formula C_6H_6. The standard quantum chemical method has been employed for hydrogen-benzene system so as to accurately determine physisorption binding energies over the high-symmetry sites. Here, we have calculated the binding energy of Hydrogen atom for three suitable positions of benzene surface. For the calculations, Counterpoise correction (CP) is employed to minimize the basis set superposition error as mentioned in [52] though the usage of CP corrections is highly debated. Calculated adsorption energies at three positions considered in Figure 1 are presented in Table 2. It is clear from Table 2 that the hollow site is the most favourable location because it has higher binding energy. In the case of H_2, only the most favourable position (h site) is employed. Binding energy values with CP corrections and without CP corrections (shown in the bracket) are shown in Table 2. In Figure 2, the structure of benzene along with the adsorption of H and H_2 in the hollow site is shown. Binding energies computed on benzene surface follow a similar trend as theoretically calculated values already presented in Table 1.

Table 2. Physisorption energy of H and H_2 on the benzene surface.

Species	Adsorption energy in h site (Kelvin)	Adsorption energy in b site (Kelvin)	Adsorption energy in c site (Kelvin)
H	217 (336*)	117	105
H_2	315 (1006*)		

* without CP.

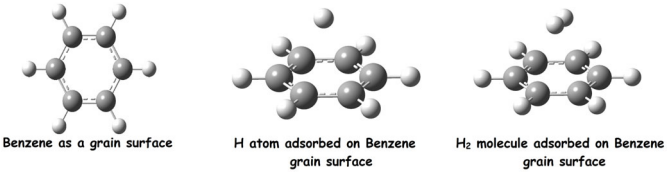

Fig. 2. Benzene as a grain surface.

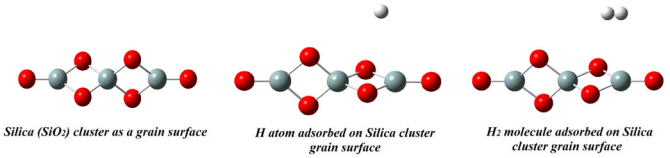

Fig. 3. Silica cluster as a grain surface.

Table 3. Adsorption energy of H and H_2 on silica surface.

Species	Energy (Kelvin)
H	580
H_2	1090

3.2 Silica cluster

Here, we calculate the binding energies of H and H_2 on bare silicate grain (a compound containing silicon). In order to mimic the realistic nature of the silicate grain, here, we consider three silica molecules together. For the better accuracy, we might have increased the size of the cluster but it would take a huge computational time to converge. Thus we have restricted ourself by considering $(SiO_2)_3$ to mimic the silicate nature of the grain surface. Figure 3 depicts the silica cluster as well as the position of adsorbed species (H and H_2) with the silica cluster. In Table 3, we have shown our calculated binding energies. Here also, we found that binding energy of H_2 is higher than that of H atom.

3.3 Water cluster

To calculate the binding energy of H and H_2, here we use the water cluster (six water molecules as a grain surface) to mimic the water ice grain. Reference [53] calculated various geometries of water clusters ($(H_2O)_n$, for n = 1–8). They found that most stable structure of the water hexamer is the chair configuration, thus, we consider the hexamer structure (chair) of the water molecule as a substrate here. Recent studies suggest that around the dense cloud region, The major portion (>70%) of the interstellar grain

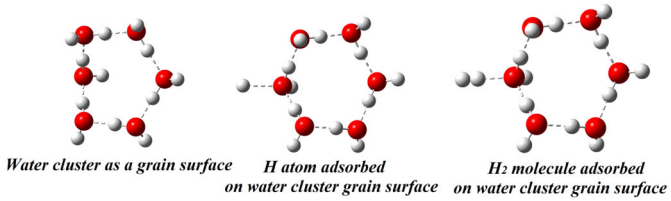

Fig. 4. Water cluster (c-hexamer chair configuration) as a grain surface.

Table 4. Adsorption energy of H and H_2 on water surface.

Species	Energy (Kelvin)
H	181
H_2	545

Table 5. Different sets of existing binding energy of H and H_2.

Species	Set 1 [55] (Kelvin)	Set 2 ([56] for olivine) (Kelvin)	Set 3 ([56] for amorphous carbon) (Kelvin)	Set 4 [57] (Kelvin)
H	350	373	658	499 ± 3
H_2	450	314	542	660 ± 6

mantle may be covered with water molecules [35,36,54] and thus the incoming gas species may be directly adsorbed onto the water ice. So, knowing the binding energies of the adsorbed species with water ice is essential to come up with a better estimation of the composition of interstellar grain mantle in dense cloud regions. Figure 4 shows the structure of the water cluster (c-hexamer chair configuration) along with the adsorbed configuration of H and H_2. Table 4 shows the calculated binding energies (no CP corrections is considered here) with the water cluster. As in the case other substrates, water cluster also yields the similar trend between the binding energies of H and H_2. We also found an interesting trend for the binding energies obtained with the size of the water cluster ($n = 1$–6). As we have increased the size of the water cluster, we have obtained the higher values of binding energies. For example, the binding energy of H and H_2 with the single water molecule ($n = 1$, monomer) is found to be 30 K and 361 K respectively, the same energy is obtained 125 K and 528 K respectively with the four water molecules ($n = 4$, c-tetramer) and with six water molecules ($n = 6$, c-hexamer chair) it is found to be 181 K and 545 K.

3.4 Binding energy already available from the earlier studies

Table 5 presents different sets of available theoretical and experimental values of binding energies of H and H_2. Set 1 corresponds to the theoretical values obtained by [55]. The desorption energies of H and H_2 are experimentally determined by [56,58] (Set 3 of Tab. 5) for amorphous carbon with values of 658 K for H and 542 K for H_2 and for olivine grain (Set 2 of Tab. 5) with values of 373 K and 314 K for H and H_2 respectively. Reference [59] calculated the van der Waals interaction between graphite and atomic hydrogen with energy 503 ± 6 K. This value fully supports the experimental data given by [57] where the best estimate was given as 499 ± 3 K. Reference [60] used DFT methods to calculate a value 400 K for H_2 interacting with carbonaceous material (carbon nanotube), while [57] gives a best estimate of 660 ± 6 K for H_2-graphite system. Estimated values of [57] are shown in Table 5 as Set 4. For molecular hydrogen, reference [61] found a large distribution of energies using TPD experiments. According to their study, the mean value of the binding energy of H_2 can be 520 K for the non-porous substrate which is very close to the theoretical value obtained by [23] of 550 K and experimental value of [62] of 550 ± 35 K, based on a mixture of water and methanol ice. Reference [63] found the value for H_2 as 440 K which was also used by [64]. For H atom on ice, there are three theoretical values for crystalline and amorphous ice: [23,65,66] determined energies of 450 K, ≈500 K and 400 ± 50 K respectively. Reference [64] used 650 K calculated by [67] for the binding energy of atomic hydrogen on amorphous ice. It is to be noted that the binding energy of H_2 molecule is less compared to that of H atom for Set 2 and Set 3 whereas for Set 1 and Set 4, the trend is opposite. Interestingly, for all our calculations, we obtained the same trend between H and H_2. Adsorption energy of H_2 is found to be always greater than that of H for all types of surfaces considered here.

4 Chemical modeling

Formation of hydrogen molecules was studied by various authors [25,26,30,32]. References [30,56] discussed the steady state conditions that may be reached by keeping the flux and temperature fixed. Here, we have used the steady state relation obtained by the earlier authors to calculate the H_2 formation efficiency window (Fig. 5) for various sets of binding energy values shown in Table 5. For this case, we consider a flux of 0.18×10^{-8} ML s^{-1} falling on a grain of diameter 0.1 μm. Density of the adsorption sites (s_n) is assumed to be 2×10^{14} cm^{-2} for the olivine surface (Set 1 and Set 2 of Tab. 5) and 5×10^{13} cm^{-2} for the amorphous carbon surface (Set 3). In case of Set 4 also, we assume $s_n = 5 \times 10^{13}$ cm^{-2}.

In case of Set 2 and Set 3, diffusion energies of atomic hydrogen were available. In case of Set 1, obtained energy against diffusion barriers was 287 K [38]. Thus the obtained ratio of the diffusion energy (E_b) and desorption energy (E_d) of atomic hydrogen for Set 2 case is ∼0.77. For Set 3, this ratio is found to be ∼0.78. This ratio is very poorly constrained in the literature and various authors approximate their choices in the range of 0.3–0.8. Since in case of Set 1 and Set 4, no values of E_b was suggested, we use $E_b = 0.75E_d$ (solid curve of Set 1 and Set 4), which is close to the experimentally obtained ratio. For another case of Set 1 and Set 4, we assume $E_b = 0.35E_d$ (dashed curves of Set 1 and Set 4). As expected, it is found that as we are increasing the mobility of the atomic hydrogen

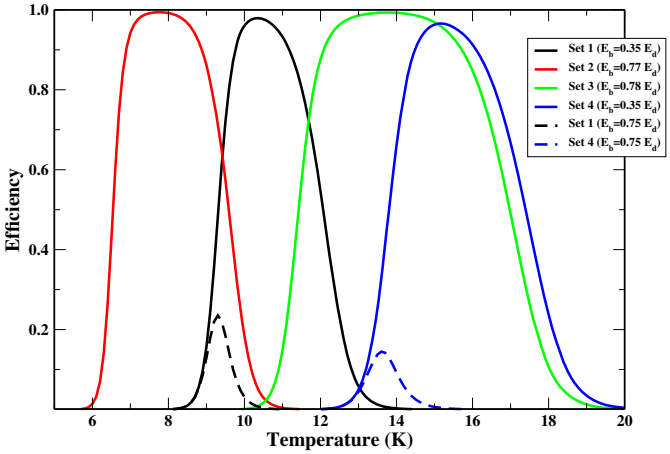

Fig. 5. Efficiency window for various sets of binding energy shown in Table 5.

(by decreasing the barrier against diffusion), the efficiency of formation increases (solid curves of Set 1 and Set 4) and hydrogen molecules are efficiently forming within the much wider zone. For the olivine grain (Set 2), H_2 formation efficiency is maximum around 8–9 K whereas for the binding energy on amorphous carbon grain (Set 3) it is around 13–14 K. Efficiency window obtained for the amorphous carbon grain (Set 3) is much wider than that of the olivine grain (Set 2). Considering the value obtained by [55] (Set 1), the H_2 formation efficiency peaks around 10 K. For the Set 4 case, the peak efficiency is obtained to be around 15 K.

5 Conclusion

We have performed ab-initio calculations for the adsorbed species on benzene, silicate cluster and water cluster systems to investigate the physisorption binding energy of hydrogen atom and molecule. Here, we have used smaller configuration of the substrate to save the computational time. The main goal of this work was to see the trend of binding energies between H and H_2. From our calculated physisorption energies of hydrogen atom and molecule on different grain surfaces, we found an interesting trend that binding energy of H_2 remains always higher than that of the H atom for all the cases. Our calculated values of the binding energies of H atom with the silica cluster and water cluster is very low as compared to the experimentally obtained values. This may be due to the fact that in case of our calculations, we are considering only one benzene, three SiO_2 and six H_2O molecules to mimic the nature of the carbonaceous, silicate and water substrate respectively which may not represent the true astrophysical scenarios. However, we believe that ours is a good starting point to consider more complex and realistic systems.

Authors contribution statement

All the authors contributed equally to the paper.

M.S. gratefully acknowledges DST, the Government of India for providing financial assistance through DST-INSPIRE Fellowship [IF160109] scheme. P.G. want to acknowledge the DST (Grant No. SB/S2/HEP-021/2013) project for their financial support. D.S. want to thank MoES project for his financial support during some part of this project work, A.D. and S.K.C. wish to acknowledge ISRO respond (Grant No. ISRO/RES/2/402/16-17) project. A.D. want to acknowledge Rajdeep Saha and Liton Majumdar for the discussions related to this paper.

References

1. V. Wakelam, I.W.M. Smith, E. Herbst, J. Troe, W. Geppert, H. Linnartz, K. Öberg, E. Roueff, M. Agúndez, P. Pernot, H.M. Cuppen, J.C. Loison, D. Talbi, Space Sci. Rev. **156**, 13 (2010)
2. S. Chakrabarti, S.K. Chakrabarti, A&A **354**, L6 (2000)
3. A. Das, S.K. Chakrabarti, K. Acharyya, S. Chakrabarti, New Astronomy **13**, 457 (2008)
4. A. Das, L. Majumdar, S.K. Chakrabarti, S. Chakrabarti, New Astronomy **23**, 118 (2013)
5. A. Das, L. Majumdar, S.K. Chakrabarti, R. Saha, S. Chakrabarti, Mon. Not. R. Astron. Soc. **433**, 3152 (2013)
6. A. Das, L. Majumdar, D. Sahu, P. Gorai, B. Sivaraman, S.K. Chakrabarti, ApJ **808**, 21 (2015)
7. A. Das, L. Majumdar, S.K. Chakrabarti, D. Sahu, New Astronomy **35**, 53 (2015)
8. S.K. Chakrabarti, L. Majumdar, A. Das, S. Chakrabarti, Astrophys. Space Sci. **357**, 90 (2015)
9. L. Majumdar, A. Das, S.K. Chakrabarti, S. Chakrabarti, Res. A&A **12**, 1613 (2012)
10. L. Majumdar, A. Das, S.K. Chakrabarti, S. Chakrabarti, New Astronomy **20**, 15 (2013)
11. L. Majumdar, A. Das, S.K. Chakrabarti, A&A **562**, A56 (2014)
12. L. Majumdar, A. Das, S.K. Chakrabarti, ApJ **782**, 73 (2014)
13. L. Majumdar, P. Gorai, A. Das, S.K. Chakrabarti, Astrophys. Space Sci. **360**, 64 (2015)
14. B. Sivaraman, N. Radhika, A. Das, G. Gopakumar, L. Majumdar, S.K. Chakrabarti, K.P. Subramanian, B.N. Raja Sekhar, M. Hada, Mon. Not. R. Astron. Soc. **448**, 1372 (2015)
15. P. Gorai, A. Das, L. Majumdar, S.K. Chakrabarti, B. Sivaraman, E. Herbst, Molecular Astrophysics (2017), doi:10.1016/j.molap.2017.01.004
16. A.G.G.M. Tielens, *The Physics and Chemistry of the Interstellar Medium* (Cambridge University Press, 2010)
17. J.M. Greenberg, Surf. Sci. **500**, 793 (2002)
18. I. Langmuir, Trans. Faraday Soc. **17**, 621 (1922)
19. D.D. Eley, E.K. Rideal, Nature **146**, 401 (1940)
20. D.D. Eley, P.R. Soc. A **178**, 452 (1941)
21. J. Harris, B. Kasemo, Surf. Sci. **105**, L281 (1981)
22. R.J. Gould, E.E. Salpeter, ApJ **138**, 393 (1963)
23. D.J. Hollenbach, E.E. Salpeter, J. Chem. Phys. **53**, 79 (1970)
24. D.J. Hollenbach, E.E. Salpeter, ApJ **163**, 155 (1971)
25. S.K. Chakrabarti, A. Das, K. Acharyya, S. Chakrabarti, A&A **457**, 167 (2006)
26. S.K. Chakrabarti, A. Das, K. Acharyya, S. Chakrabarti, Bull. Astr. Soc. India **34**, 299 (2006)

27. D.A. Williams, Faraday Discuss **109**, 1 (1998)
28. D.A. Williams, Surf. Sci. **500**, 823 (2002)
29. A. Hu, W.W. Duley, ApJ **660**, L137 (2007)
30. O. Biham, I. Furman, V. Pirronello, G. Vidali, ApJ **553**, 595 (2001)
31. Q. Chang, H.M. Cuppen, E. Herbst, A&A **434**, 599 (2005)
32. D. Sahu, A. Das, L. Majumdar, S.K. Chakrabarti, New Astronomy **38**, 23 (2015)
33. A.G.G.M. Tielens, W. Hagen, A&A **114**, 245 (1982)
34. A. Das, K. Acharyya, S. Chakrabarti, S.K. Chakrabarti, A&A **486**, 209 (2008)
35. A. Das, K. Acharyya, S.K. Chakrabarti, Mon. Not. R. Astron. Soc. **409**, 789 (2010)
36. A. Das, S.K. Chakrabarti, Mon. Not. R. Astron. Soc. **418**, 545 (2011)
37. S. Viti, Astron. Geophys. **48**, 25 (2007)
38. V. Pirronello, C. Liu, L.Y. Shen, G. Vidali, ApJ **475**, L69 (1997)
39. G. Vidali, J.E. Roser, G. Manico, V. Pirronello, Adv. Space Res. **33**, 6 (2004)
40. G. Vidali, J.E. Roser, L. Ling, E. Congiu, G. Manicó, V. Pirronello, Faraday Discuss **133**, 125 (2006)
41. H.J. Fraser, S.E. Bisschop, K.M. Pontoppidan, A.G.G.M. Tielens, E.F. van Dishoeck, Mon. Not. R. Astron. Soc. **356**, 125 (2005)
42. N. Watanabe, A. Nagaoka, T. Shiraki, A. Kouchi, ApJ **616**, 638 (2004)
43. A. Galano, J. Phys. Chem. A **111**, 1677 (2007)
44. M. Bonfanti, R. Martinazzo, G.F. Tantardini, A. Ponti, J. Phys. Chem. C **111**, 5825 (2007)
45. G. Forte, A. Grassi, G.M. Lombardo, A. La Magna, G.G.N. Angilell, R. Pucci, R. Vilardi, Phys. Lett. A **372**, 6168 (2008)
46. J. Petucci, C. LeBlond, M. Karimi, G. Vidali, J. Chem. Phys. **139**, 044706 (2013)
47. M.J. Frisch, G.W. Trucks, H.B. Schlegel et al., G09:RevC.01, Gaussian, Inc., Wallingford CT (2013)
48. T.H. Dunning Jr., J. Chem. Phys. **90** 1007 (1989)
49. N.N. Avgul, A.A. Isirikyan, A.V. Kiselev, I.A. Lygina D.P. Poshkus, Russ. Chem. Bull. **6**, 1334 (1957)
50. N.N. Avgul, A.V. Kiselev, I.A. Lygina, D.P. Poshkus, Russ. Chem. Bull. **8**, 1155 (1959)
51. R. Barrer, Proc. Royal Soc. **A161**, 476 (1937)
52. S.F. Boys, S. Bernardi, Mol. Phys. **19**, 553 (1970)
53. K. Ohno, M. Okimura, N. Akaib, Y. Katsumotoa, Phys. Chem. Chem. Phys. **7**, 3005 (2005)
54. A. Das, D. Sahu, L. Majumdar, S.K. Chakrabarti, Mon. Not. R. Astron. Soc. **455**, 540 (2016)
55. M. Allen, G.W. Robinson, ApJ **212**, 396 (1977)
56. N. Katz, I. Furmann, O. Biham, V. Pironello, G. Vidali, ApJ **522**, 305 (1999)
57. G. Vidali, G. Ihm, H.-Y. Kim, M.W. Cole, Surf. Sci. Rep. **12**, 133 (1991)
58. V. Pirronello, C. Liu, J.E. Roser, G. Vidali, A&A **344**, 681 (1999)
59. E. Ghio, L. Mattera, C. Salvo, F. Tommasini, U. Valbusa, J. Chem. Phys **73**, 556 (1980)
60. S. Han, H.M. Lee, Carbon **42**, 2169 (2004)
61. F. Dulieu, L. Amiaud, S. Baouche, A. Momeni, J.-H. Fillion, J.L. Lemaire, Chem. Phys. Lett. **404**, 187 (2005)
62. S.A. Sandford, L.J. Allamandola, ApJ **409**, L65 (1993)
63. L. Hornekaer, A. Baurichter, V.V. Petrunin, A.C. Luntz, B.D. Kay, A. Al-Halabi, J. Chem. Phys. **122**, 124701 (2005)
64. H. Cuppen, L. Hornekaer, J. Chem. Phys. **128**, 174707 (2008)
65. V. Buch, R. Czerminski, J. Chem. Phys. **95**, 6026 (1991)
66. A. Al-Halabi, A. Kleyn, E.F. van Dishoeck, G.J. Kroes, J. Phys. Chem. B **106**, 6515 (2002)
67. A. Al-Halabi, E.F. van Dishoek, Mon. Not. R. Astron. Soc. **382**, 1648 (2007)